Rev. Adv. Mater. Sci. 33 (2013) 316-321

THE STATIC COMPRESSIVE BEHAVIOR OF ALUMINUM FOAM

Xinzhu Wang[1] and Guangtao Zhou[2]

[1]State Key Laboratory of Coal Mine Disaster, Dynamics and Control, Department of Engineering Mechanics, Chongqing University, Chongqing 400040, China
[2]College of Mechanical Engineering and automation, Huaqiao University, Xiamen 361021, China

Received: October 17, 2011

Abstract. Failure of metal foams caused by compression is very common in practice, such as light-weight structural sandwich panels, packing materials and energy absorbing devices. In this paper, the uniaxial compression and indentation response of the closed-cell aluminum foams were investigated experimentally under quasi-static loading conditions. The indentation deformation was found to be almost totally restricted to a spherical cap-shape compacted zone under the indenter. The indentation strength of the closed-cell Al foam is larger than the uniaxial compressive strength because of the work done in tearing cell walls around the perimeter of the indenter and because of friction. The closed-cell Al foam exhibits an elastic-plastic type behavior under transverse uniaxial compressive loads. A long flat stress-strain curve shows that metal foam is a good energy absorption material.

1. INTRODUCTION

As a new multi-function engineering material, metal foams have many useful properties such as low density, high stiffness, good impact resistance, high energy absorption capacity, easy to manufacture into complex shape, good erosion resistance, etc and they can be used in applications such as light-weight sandwich panels, packing material, energy absorbing devices, structural members in air and spacecraft, and even in biomedical prosthesis [1-3]. With the development of manufacture technology, metal foams are now less costly and an increasingly large number of researchers are interested in their properties and potential engineering applications.

The compression and indentation behaviors of metal foams have been widely investigated in the recent years. Many of these works are studies experimentally on the behavior of metal foam. Wang et al. [4] also investigated the effects of cell sizes on the compressive strength and energy absorption. Zhou et al. [5] employed an ex situ SEM technique that the tested sample was moved to SEM and examined after each loading-unloading cycle, to study the compression mechanical properties of open-cell Al foams. Fleck and co-workers [6,7] performed the axisymmetric compressive tests with three types of aluminum foams: Alporas foams, Duocel foam, and Alulight foams. The experimental data shows that their self-similar model can predict the stress–strain response with a reasonable accuracy and that the differential hardening model can give a higher level of accuracy for proportional loading paths. Nieh et al. [8] studied the effects of cell morphology on the compressive properties of open-cell aluminum foams.

The finite element method was used to simulate the deformation during indentation. In recent years, several works have been published on the modeling of indentation behavior of cellular materials [9–11]. In these simulations, however, the foams were treated either as a continuum, thus they were

Corresponding author: Xinzhu Wang, e -mail: wxz@cqu.edu.cn

assumed to behave as a homogeneous bulk material, the parameters of which correspond to the average parameters of the foam or as honeycomb. Andrews et al. [12] investigated the size-dependence of the plastic strength of metallic foams and found that the indentation stress varies with the indenter diameter, showing a size effect. A simple model gives a good description of the data. Dynamic indentation and penetration tests by Ramachandra et al. [13] and Li et al. [14] showed that the indentation resistance increased significantly at velocities greater than 10 m/s. Sudheer et al. [15] experimentally investigated the deep indentation response of a closed-cell aluminum foam under different rates of penetration. Deep indentation with SEP and FEP indenters conducted on a closed-cell aluminum foam at varying penetration rates shows a gradual increase in the plastic collapse strength as well as the energy absorbed with increasing displacement rate.

The main purpose of this research is to investigate compressive response of Al foam by uniaxial compression and indentation tests. In the following, first, we describe the materials; experimental procedures adopted and then discuss indentation and compressive response along with observed failure modes in the results and discussion section.

2. SPECIMEN PREPARATION AND EXPERIMENTS

2.1. Specimen preparation

An available closed-cell aluminum foam was used in this study. It was fabricated using the direct foaming technique that uses TiH_2 powders as an additive to the molten metal for foaming. The foam has an average cell size of 2 mm with a relative density of 0.09. Cell wall thickness of the foam ranged from 80 to 100 μm. Typical macroscopic view of the foam is shown in Fig. 1. As seen from the figure, the cell sizes for this particular metal foam are very inhomogeneous locally, but have an overall uniform morphology. A foam panels was cut using an electric discharge machine to make individual 100×100×15 mm^3 specimens for compressive and indentation testing.

2.2. Test procedures

All testing was conducted on a machine with a 50 KN INSTRON 5569 universal testing machine with 10 KN load cell at room temperature (23 °C). Calibration/Verification of both the displacement of the INSTRON machine and the load detection of

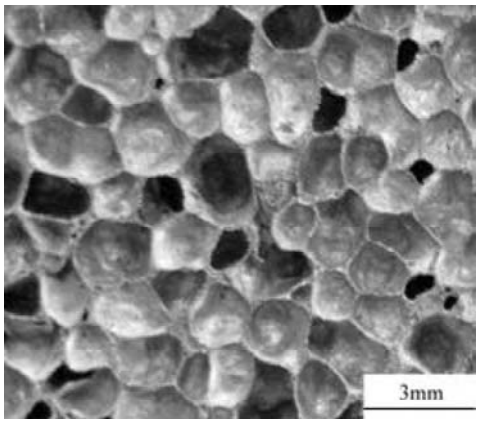

Fig. 1. Macroscopic view of the closed-cell Al foam, used in the current study.

the load cell was conducted prior to testing. The tests were carried out under displacement control at a constant loading rate. In all cases, the plate thickness orientation of the metal foam coincides with the loading direction.

During the testing, the load and crosshead displacements were recorded for both loading and unloading phases. Five specimens of each test were tested.

2.2.1. Static Indentation tests

The purpose of the static indentation tests is to find the contact stiffness of the metal foam. The diameter of the rigid spherical indenter is 2*a*=12 mm. Note that, 2*a* is equal to six to seven times the average cell diameter whereas the projected area covers 40 cells, thus ensuring the measured response is representative of the average response of the material. This relatively small indentor radius was chosen because it was desirable that the contact

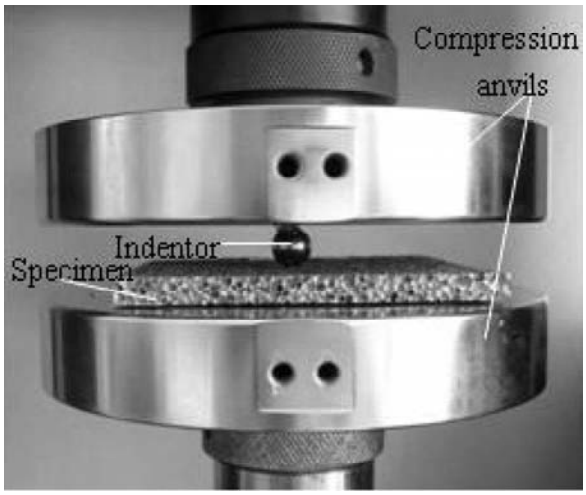

Fig. 2. Indentation test setup.

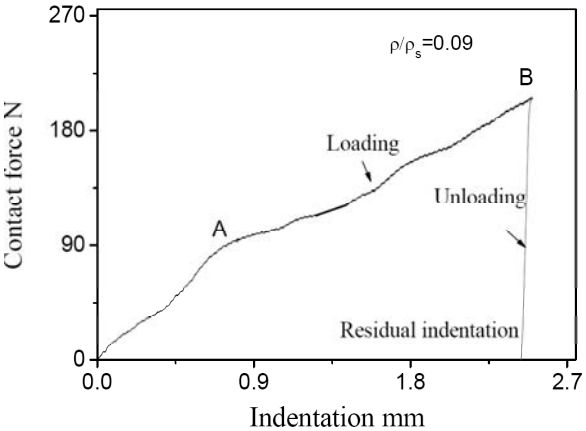

Fig. 3. Elastic-plastic response of Al foam subjected to a static indentation by a rigid steel.

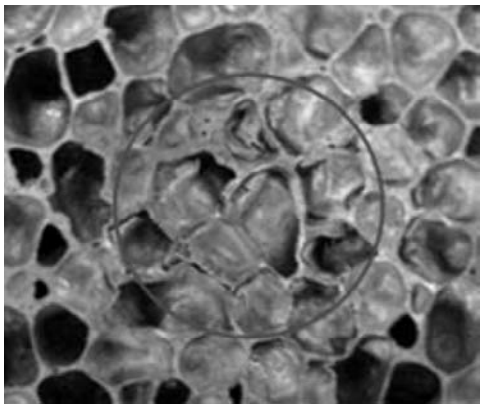

Fig. 4. Photograph of top of typical crushed Al foam.

between the indentor and the specimen could be considered as a line load. To minimise the effects of friction, the indenters were lubricated with PTFE spray.

During the experiment, the specimens were supported by a rigid steel continuous substrate in order to limit the global bending deformations. Fig. 2 shows a schematic of the indentation test setup. The tests were carried out under displacement control at a constant loading rate of 1 mm/min up to a given indentation (2.5 mm). The force to cause a specific compressive strain, e.g. 25%, is used as a measure of metal foam stiffness, then the load was released. The displacement, when the load dropped

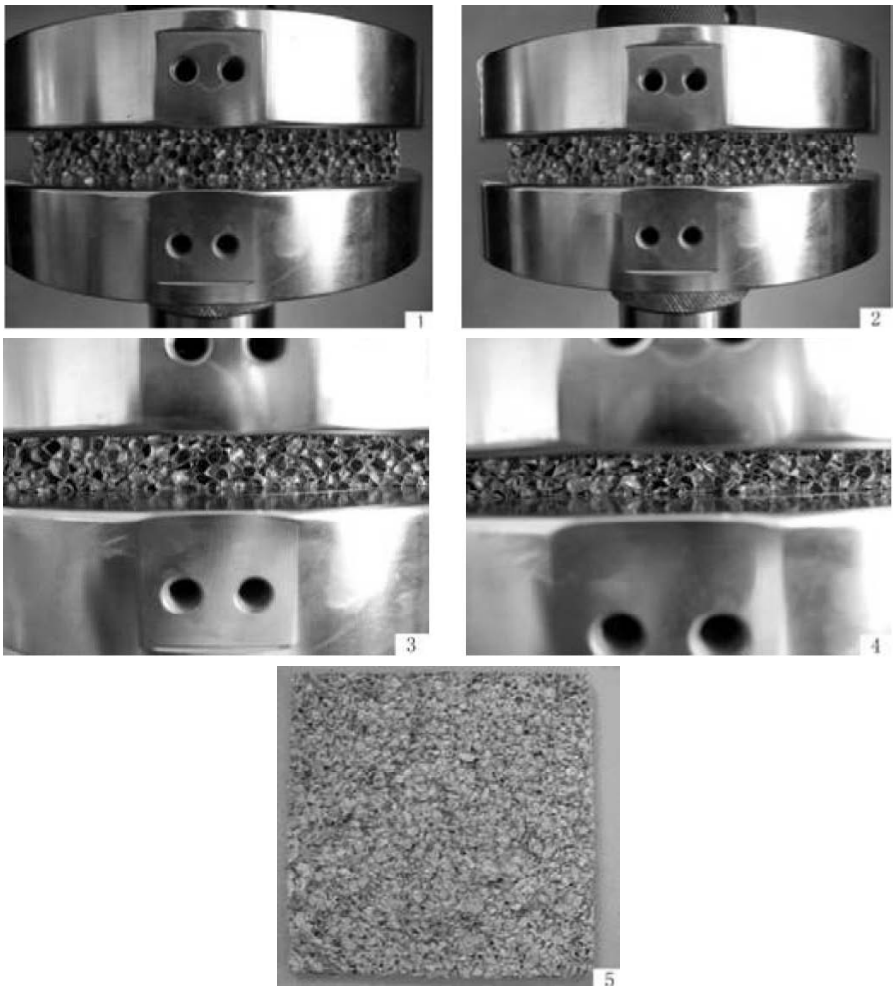

Fig. 5. Photographs of the metal foam during crushing.

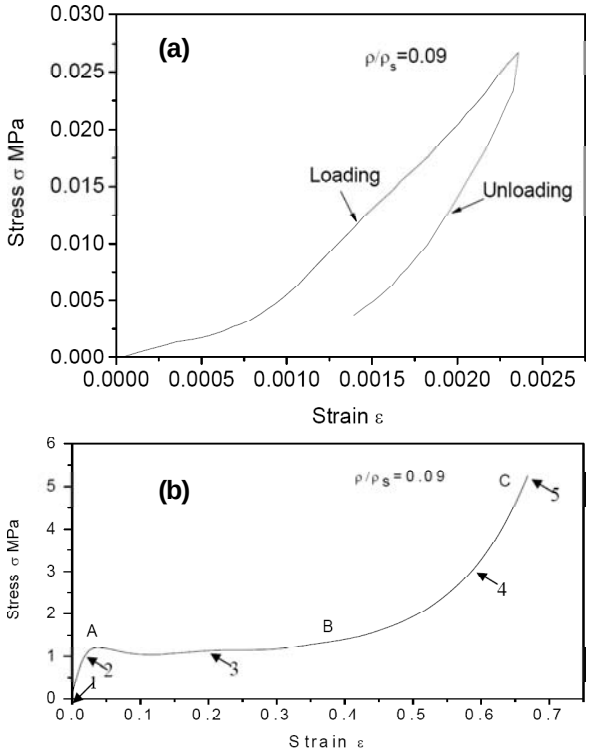

Fig. 6. Stress-strain curve from a uniaxial compression test on a typical closed-cell Al foam: (a) loading-unloading stress–strain response; (b) Compressive stress–strain response.

to zero, was considered as the residual dent magnitude. A typical load–indentation depth curve is shown in Fig. 3. Photograph of top of typical crushed Al foam showing elliptical indentation caused by a hemispherical indenter as shown Fig. 4.

2.2.2. Uniaxial compression tests

In order to study the non-linear behavior of the metal foam material, uniaxial compression test was carried out. The minimum dimension of the specimen should be at least seven times the cell size to avoid size effects. All compression tests were conducted in this direction according to ASTM C365-05 standard [16]. Specimens were placed on the bottom ram of the machine and load was applied to the specimens when the top ram moved downward at a constant speed of 0.5 mm/min. Teflon spray was used to lubricate the contact surfaces between the specimens and platens to reduce friction.

Due to stress concentrations caused by defects in the cellular structure of the aluminum foams, a small amount of plastic deformation can occur even at a very low stress level. The slope of the loading stress-strain curve is therefore not a true representation of the elastic modulus. The unloading slope, however, remains roughly constant until the foam has been loaded to its plastic collapse stress. Therefore, the young's modulus *E* was taken as the unloading modulus measured from specified fraction, 0.2%, of strain. It is conventional to convert load-displacement curves into stress-strain curves by defining stress as load divided by cross-sectional area and strain as change in specimen height divided by the undeformed height. The typical loading-unloading stress–strain and loading stress–strain relationship, deduced from the compression test, are shown in Figs. 5a and 5b. Fig. 6 shows a set of photographs of the specimen during crushing. A separate video camera was used to observe the deformation of the cells on one of the free surfaces of the block.

3. ANALYSIS AND DISCUSSION

3.1. Indentation test

Due to the elastic–plastic behavior of the metal foam the load–indentation curves have a generally non-linear shape as shown in Fig. 3. At the beginning of the testing, when the indentation magnitude is low, the load–indentation response is linear. This behavior continues until the moment when an initiation of plastic deformation (crushing of the metal foam) is triggered. After that, the load–indentation curve becomes non-linear with a rather fast continuous degradation of the specimen stiffness. Thus, the non-linear behavior is induced by the progressive crushing of the metal foam underneath the spherical indentor. The load–indentation response of the specimen at unloading phase has a less pronounced non-linear character, compared to the loading (indentation) phase. An instant magnitude of a residual dent in the specimen was measured at a zero load (Fig. 3). The oscillations in the load-indentation response are due to repeating cycles of yield, collapse and densification.

The indentation process in metal foam strongly depends upon the mechanical properties of the foam material. It should be mentioned that the mechanical behavior of rigid closed-cell materials is different compared to that of the traditional structural materials (like steel, for instance), due mainly to the plastic compressibility of the metal foams.

The total force on indenter is the sum of that to crush the Al foam beneath the indenter and that required to tear it at the edges of the indenter, that is

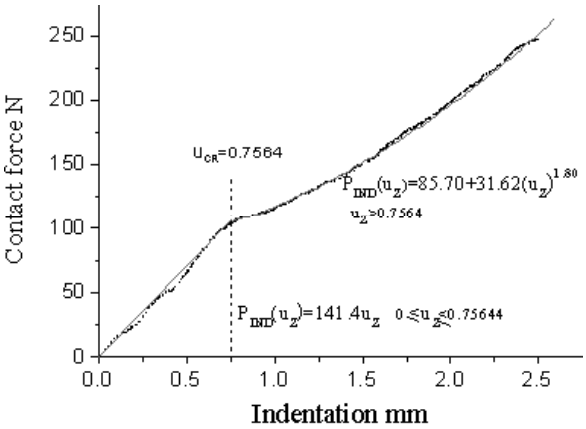

Fig. 7. Experimental data and curve fit of indentation laws for Al foam.

$$F = F_{\text{crushing}} + F_{\text{tearing}}, \tag{1}$$

where F_{crushing} is the force needed to crush the Al foam beneath the indenter, F_{tearing} is that required to tear the cells around the edge of the indenter.

The loading response of the metal foam panels can be divided into an initial elastic response and a subsequent non –linear response. The contact laws for these two stages of loading are given by Eq. (2)

$$P(u) = \begin{cases} C_0 u_z & 0 \le u_z \le u_{CR} \\ C_1 + C_2 u_z^{C_3} & u_{CR} \le u_z \le u_1 \end{cases}, \tag{2}$$

where, C_0, C_1, C_2, and C_3 are coefficients obtained by curve fitting the experimental data. u_{CR} is the intercept point of the elastic and the inelastic non-linear regions. u_1 = 2.5 mm. The experimental data was curve fit with the above equations using the graphing computer program. A typical curve fit of the experimental data during the loading phase is shown in Fig. 6. It can be observed that the experimental data in the initial elastic region is strictly non-linear in nature, but it was assumed linear for comparison purposes only.

4.2. Compressive test

The slope of the initial loading portion of the curve is lower than that of the unloading curve. As a result, measurements of young's modulus should be made from the slope of the unloading curve, as shown in Fig. 3a.

Al foam material deformed with the three steps during uniaxial compression. Fig. 3b shows the schematic diagram of this phenomenon. The 1st step is linear elasticity following the Hooke's law. The 2nd step is collapse plateau. Here, the plastic deformation and the fracture of cell wall are progressed simultaneouslya distinct peak followed by a small stress drop. So, the stress generated in the 2nd step is not increased after reaching the yielding point. This region is called as the collapse plateau region. On the other hand, it was well known that the mechanical property of aluminum foamed depends on the cell types (the closed cell and open cell), aspect ratio, cell size and its volume fraction, and degree of its dispersion. The final step is densification. The foamed aluminum deforms as a solid material.

The plastic collapse stress, σ^*_{pl} was measured as the initial peak stress reached before the onset of plastic collapse if there is one; otherwise, it is taken to be the stress at the intersection of two slopes: that for the initial loading and that for the stress plateau. The plateau stress σ_{pl} and densification strain, ε_d are also obtained from those compression tests. The plateau stress σ_{pl} and densification strain, ε_d of metal foam are extracted from the axial compression test.

Note that in Fig. 4, initially, during the stable branch of the response, the material deforms nearly uniformly. Following the local stress maximum the specimen buckles in an overall manner which can be seen in the configurations as a bowing of the edges on the left and right. This involves local distortion of the cells. As compression progresses, deformation localizes in a banded manner. The bands showed up at what is best described as randomly located sites on the cross section monitored while prevalent characteristic orientation could not be identified. The number of bands grew with time while the stress remained essentially unchanged. At other sites bands broadened and coalesced with neighboring ones. This surface deformation pattern is qualitatively similar to that reported in Wang et al. [4] who used a digital image correlation technique to establish the evolution of events. Although surface deformation patterns do not necessarily represent bulk material behavior, the randomness of the locations of bands is a distinctly different feature

Table 1. Compressive test results of metal foam specimens.

Specimen	E	σ^*_{pl}	σ_{pl}	ε_d
Value	23.8 MPa	1.19 MPa	1.12 MPa	0.531

from the one or two well-defined collapse fronts seen in in-plane crushing experiments on honeycombs. This may be a characteristic of the more complex space filling foam microstructure but, more probably, is due to the more random distribution of larger geometric irregularities in foams than in the polymeric honeycomb of Papka and Kyriakides. Despite this difference, during the main evolution of localized deformation, the stress traced essentially a plateau in both cases. At an average ''strain'' of about 45%, the response develops a positive slope once more.

The average young's modulus *E*, the plastic collapse stress, σ^*_{pl}, the plateau stress σ_{pl} and densification strain, ε_d of metal foam are illustrated in Table 1.

Motivated by the observation of Sugimura et al. [9], who found that tangent modulus measured from the unloading data is appreciably higher than the initial loading slope, slopes of the initial loading as well as the unloading (past the yield) stress–strain curves were measured. For consistency, the tangent moduli during loading and unloading, EL and EUL, were always estimated by fitting a linear curve to the stress–strain data obtained between the stress levels of 0.5–1.0 MPa.

5. CONCLUSIONS

In this paper, a brief review of metal foam compressive behavior was presented first. Then the compressive test and indentation was introduced. Foam collapsing and tearing at the periphery of indenter were found to be the failure mechanism for samples with a rigid spherical indenter. The indentation deformation was found to be almost totally restricted to a spherical cap-shape compacted zone under the indenter. Al foam exhibits an elastic-plastic type behavior under transverse compressive loads. A long flat stress-strain curve shows that metal foam is a good energy absorption material. The indentation strength of Al foam is larger than the uniaxial compressive strength because of the work done in tearing cell walls around the perimeter of the indenter and because of friction.

ACKNOWLEDGMENT

This work are performed with the financial support by the Key Project of Chinese Ministry of Education (No. 313059), the Fundamental Research Funds for the Central Universities (Project No. CDJRC-10240002, CDJZR12240067, CDJZR1224071, CDJZR12248801, CDJZR12110072), China Postdoctoral Science Foundation (No. 2011M500067).

REFERENCES

[1] L.J. Gibson and M.F. Ashby, *Cellular solids: structure and properties. 2nd ed.* (Cambridge University Press, Cambridge, 1997).
[2] J. Banhart // *Prog. Mater. Sci.* **46** (2001) 559.
[3] H.P. Degischer and B. Kriszt, *Handbook of cellular metals: production, processing, applications* (Wiley-VCH Verlag, Weinheim, 2002).
[4] B.Wang, D.He and G.Shu, In: *Metal Foams and Porous Metal Structures* (MIT Verlag, 2001), p. 351.
[5] J. Zhou, P. Shrotriya and W.O. Soboyejo // *Mech. Mater.* **36** (2004) 781.
[6] V.S. Deshpande and N.A. Fleck // *J. Mech. Phys. Solids.* **48** (2000) 1253.
[7] I. Sridhar and N.A. Fleck // *J. Mater. Sci.* **40** (2005) 4005.
[8] T.G. Nieh, K. Higashi and J. Wadsworth // *Materials Science and Engineering A.* **283** (2000) 105.
[9] R.E. Miller // *Int. J. Mech. Sci.* **42** (2000) 729.
[10] A. Gilchrist and N.J. Mills // *Int. J. Imp. Eng.* **25** (2001) 767.
[11] A.E. Markaki and T.W. Clyne // *Acta Mater.* **49** (2001) 1677.
[12] E.W. Andrews, G. Gioux, P. Onck and L.J. Gibson // *Int. J. Mechanical Sciences* **43** (2001) 701.
[13] S. Ramachandra, P. Sudheer and U. Ramamurty // *Scripta Materialia* **49** (2003) 741.
[14] Q.M. Li, R.N. Maharaj and S.R. Reid // *Materials Science and Engineering* **37** (2003175.
[15] P. Sudheer Kumar, S. Ramachandra and U. Ramamurty // *Materials Science and Engineering A* **347** (2003) 330.
[16] *ASTM C365-05. Standard Test Method for Flatwise Compressive Properties of Sandwich Cores. Annual book of the ASTM standards* (American Society for Testing and Materials: Philadelphia, PA).